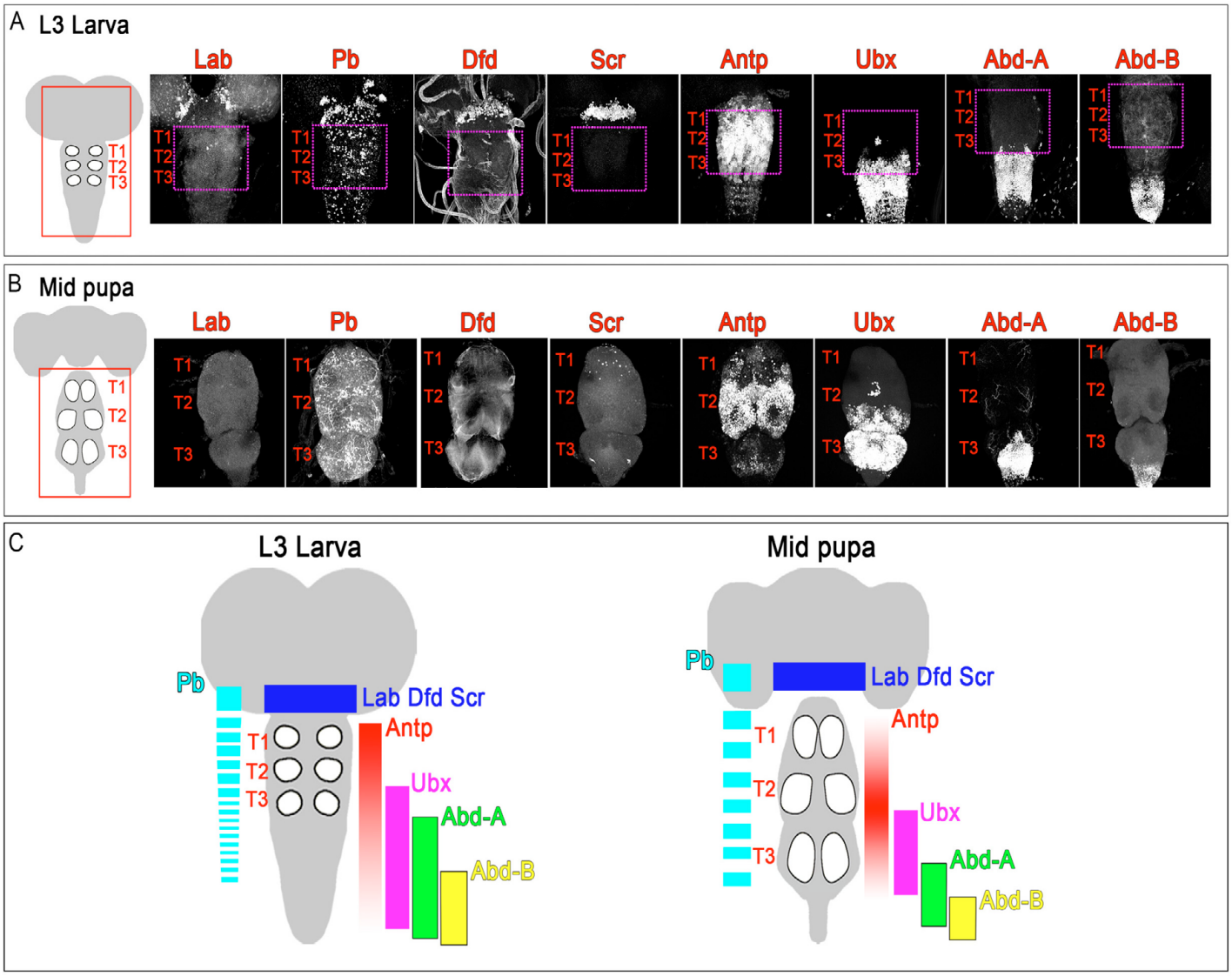

Fig. S1. Hox expression patterns during late larval and mid-pupal stages. (**A**,**B**) Antibody stains of dissected VNCs for each of the eight Hox proteins. Entire *z*-stack images are merged using ImageJ except Dfd, which produced high background. Thoracic segments T1 to T3 are marked with purple dotted boxes. (A) Late L3 larval stage (~120 hour AEL). (B) Mid-pupa (3-4 day APF) stage. (**C**) Schematic summary of Hox expression patterns; the white circles represent the thoracic neuropils. Antp, Ubx and Pb are expressed in the thoracic segments.

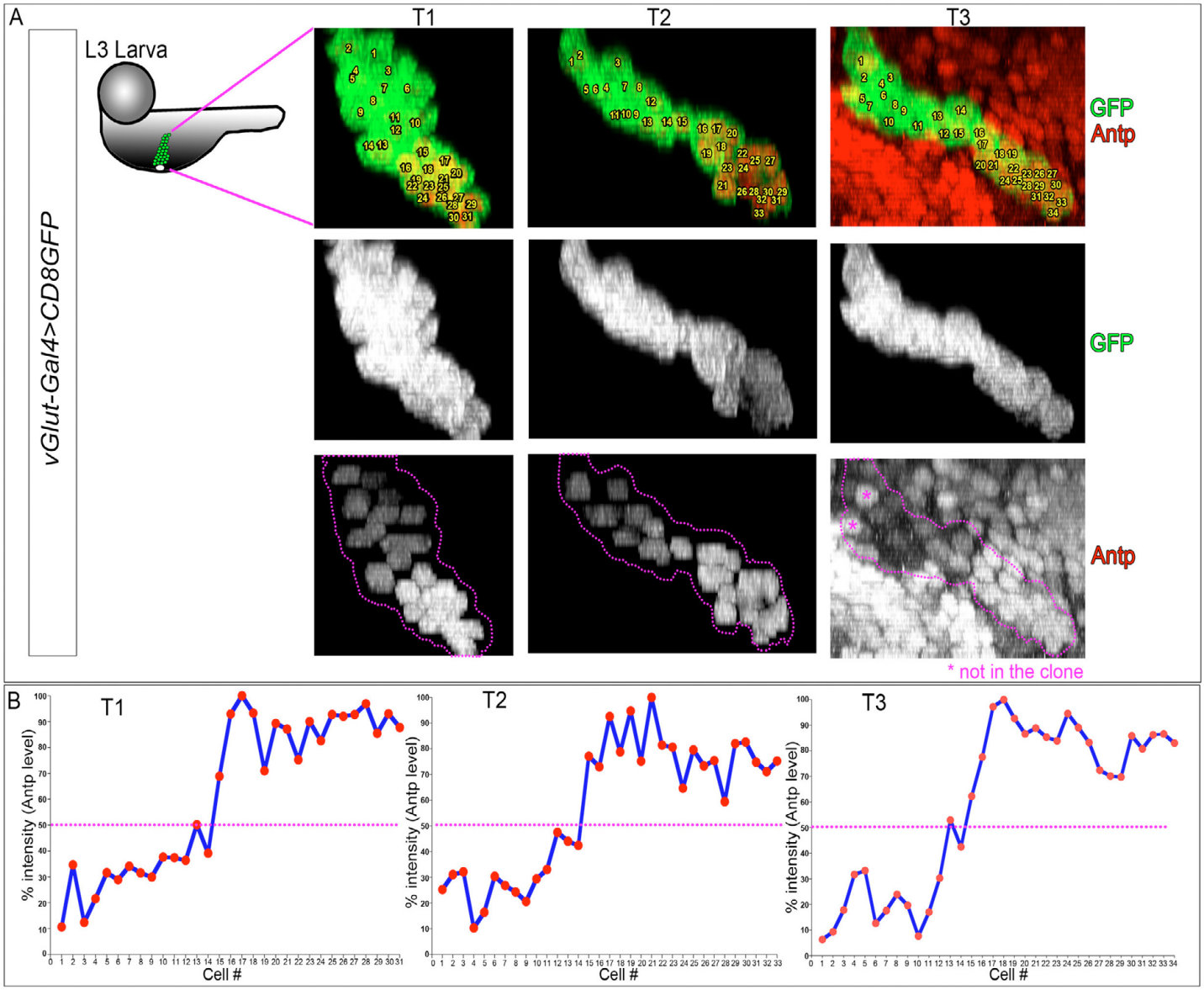

Fig. S2. Quantification of Antp expression levels in the larval LinA MNs. LinA MARCM clones in late L3 larva (~120 hour AEL) labeled with *vGlut-Gal4 >CD8GFP* (green). (**A**) Merged images from the sagittal re-sliced images shown in Fig. 2B. From left to right: T1, T2 and T3 LinA clones stained for Antp (red). To visualize more clearly Antp expression levels, non-clonal regions were removed in T1 and T2 images. Merged images with cell numbers assigned by their relative cell body positions from dorsal (1) to ventral (2) positions along the VNC are shown. The LinA clones are outlined with pink dotted lines (bottom). (**B**) Quantification of the Antp expression levels in individual cells in each LinA clone shown in A. From left to right: T1, T2 and T3 LinA clones. Each point represents an individual cell's Antp intensity relative to the maximum intensity in each LinA clone. The 50% region is marked by pink dotted lines.

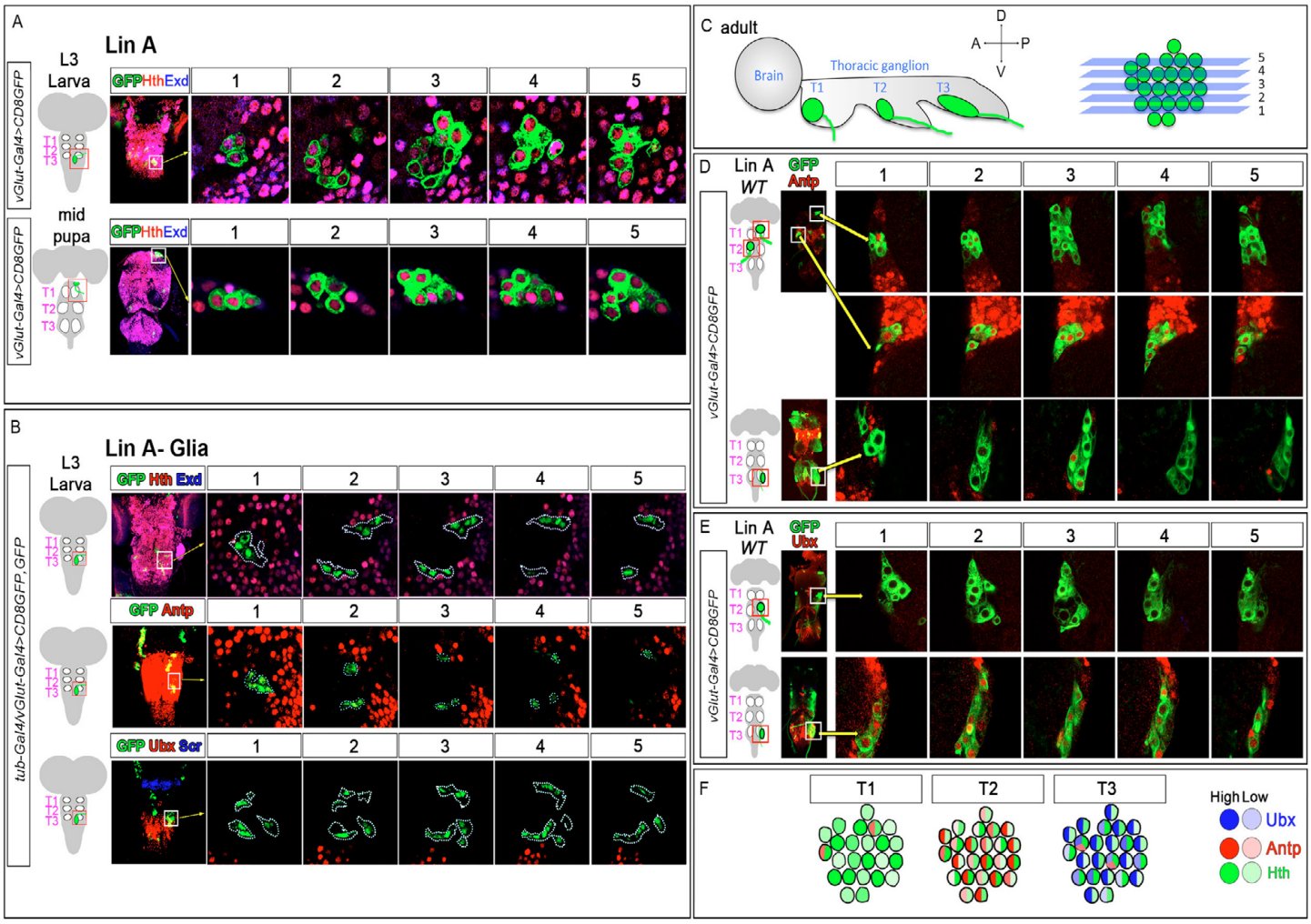

Fig. S3. Expression patterns of Hox and Hox co-factors in LinA progeny. (**A**,**B**) Expression patterns of Hox co-factors in LinA MNs and Hox and Hox co-factors LinA glia. 1 to 5 represent individual *z*-stack slices from ventral to dorsal, respectively. (A) Shown are LinA MARCM clones labeled with *vGlut-Gal4 >CD8GFP* (green). L3 (120 hour AEL; top) or mid-pupa (~3-4 days APF; bottom) VNCs were Lin A MARCM clones co-stained for Hth (red) and Exd (blue). Hth and Exd are both detected in all LinA MNs but at variable levels. (B) L3 stage LinA MARCM clones labeled with *tub-Gal4*; *vGlut-Gal4 >CD8GFP* (green). LinA-derived glia, identified by their position in the VNC, are outlined in light blue dotted lines. Antp is expressed weakly in a subset of LinA-derived glia. (**C-F**) Expression patterns of Hox and Hox co-factors in LinA MNs in the adult. (C) Schematic represenation of LinA in the adult VNC. (D,E) LinA MARCM clones stained for Antp (D) and Ubx (E) in the adult labeled with *vGlut-Gal4 >CD8GFP* (green). Five *z*-stack slices from dorsal (1) to ventral (5) along the VNC are shown. (D) LinA clones in T1 (top row), T2 (middle row) and T3 (bottom row) stained for Antp (red). Antp is seen in a small number of cells in T1, T2 and T3. (E) LinA clones in T2 and T3 stained for Ubx (red). Ubx is present in most cells in T3, but not in T2. (F) Summary of Hox expression patterns in LinA MN progeny in the adult. Hth is expressed in all LinA-derived MNs in all three segments (data not shown). Antp is expressed strongly in all T2 LinA MNs, but only about two or three MNs in T1 and T3. Ubx is expressed in most LinA-derived MNs in T3, but not in T1 or T2.

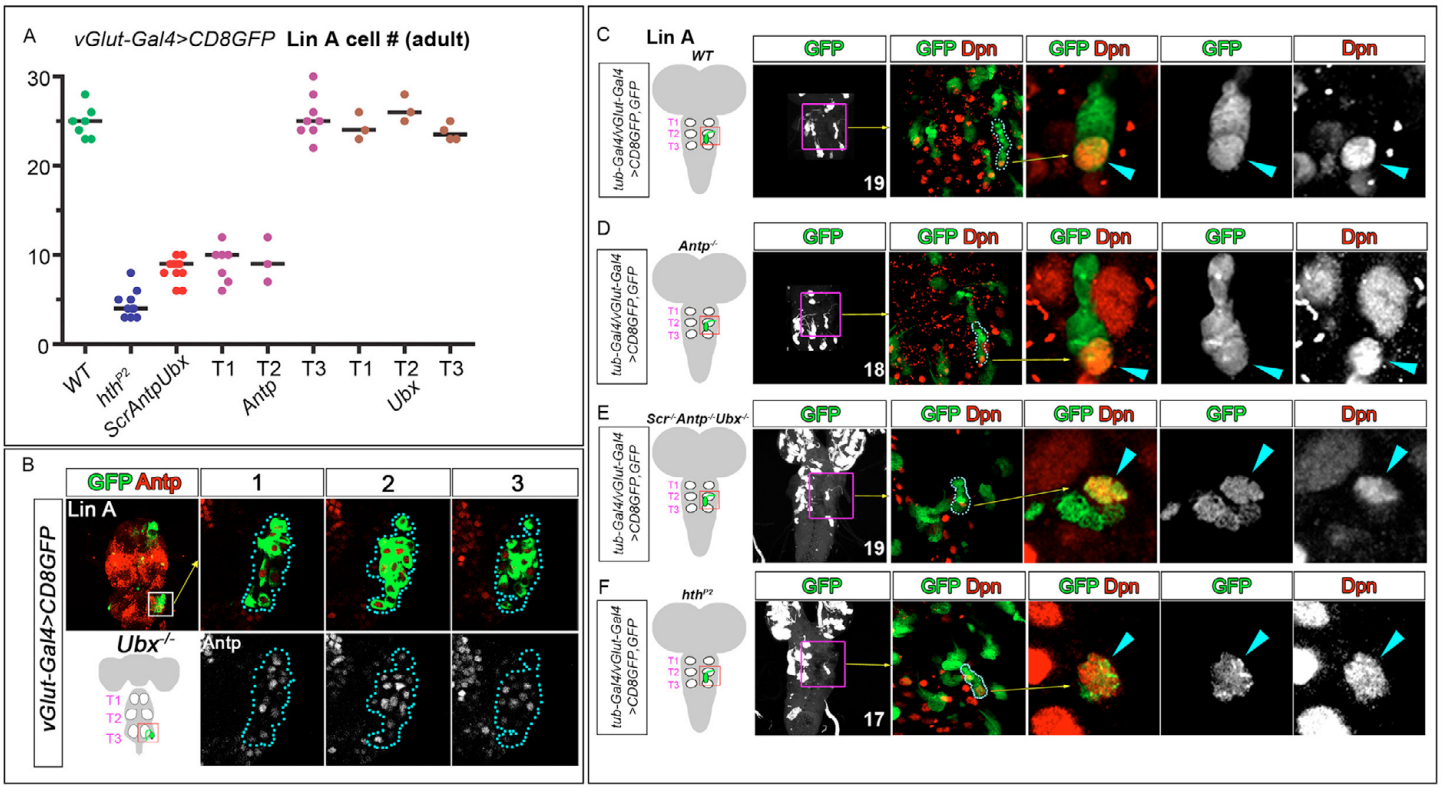

Fig. S4. Hox and *hth* are required for the survival of LinA progeny. (**A**) Quantification of leg motor neurons at the adult stage. Each data point represents the number of neurons in a single LinA MARCM clone labeled with *vGlut-Gal4 >CD8GFP.* Median values are indicated by black bars. Data for all three thoracic segments are pooled for WT, *hth*, and *Scr Antp Ubx*, and are shown separately for *Antp* and *Ubx* mutant clones. *Antp* reduces MN number in T1 and T2, but not T3. *Ubx* mutants alone have no effect on MN number. (**B**) *Ubx* mutant LinA clones labeled with *vGlut-Gal4 >CD8GFP* (green) at the mid pupa stage. LinA clones are outlined in light blue dotted lines. 1 to 3 represent individual *z*-stack slices from ventral to dorsal, respectively. Antp (red) is ectopically expressed in the *Ubx* mutant T3 LinA MNs. (**C-F**) LinA NB and progeny in Hox and *hth* mutant clones during early third instar stages. LinA clones in early third instar (82-92 hours AEL) VNCs labeled with *tub-Gal4*; *vGlut-Gal4 >CD8GFP* (green) and stained for Dpn (red), a NB marker. The clones are shown at three magnifications: the left-most images show the entire VNC (non LinA MNs are removed for visualizing LinA clones clearly using imageJ; magnified regions are marked by magenta boxes); images second from the left show the clone region (LinA clones are outlined with light blue dotted lines), and the three images on the right show a single *z*-stack slice through the clone. LinA NBs are indicated by light-blue arrowheads. The number of progeny associated with each clone, counted by the number of Elav+ cells (not shown), is shown in the lower right-hand corner of the low magnification images. (C) WT, (D) $Antp^{-/-}$, (E) $Scr^{-/-}$ $Antp^{-/-}$ $Ubx^{-/-}$, (F) hth^{P2} mutant LinA clones.

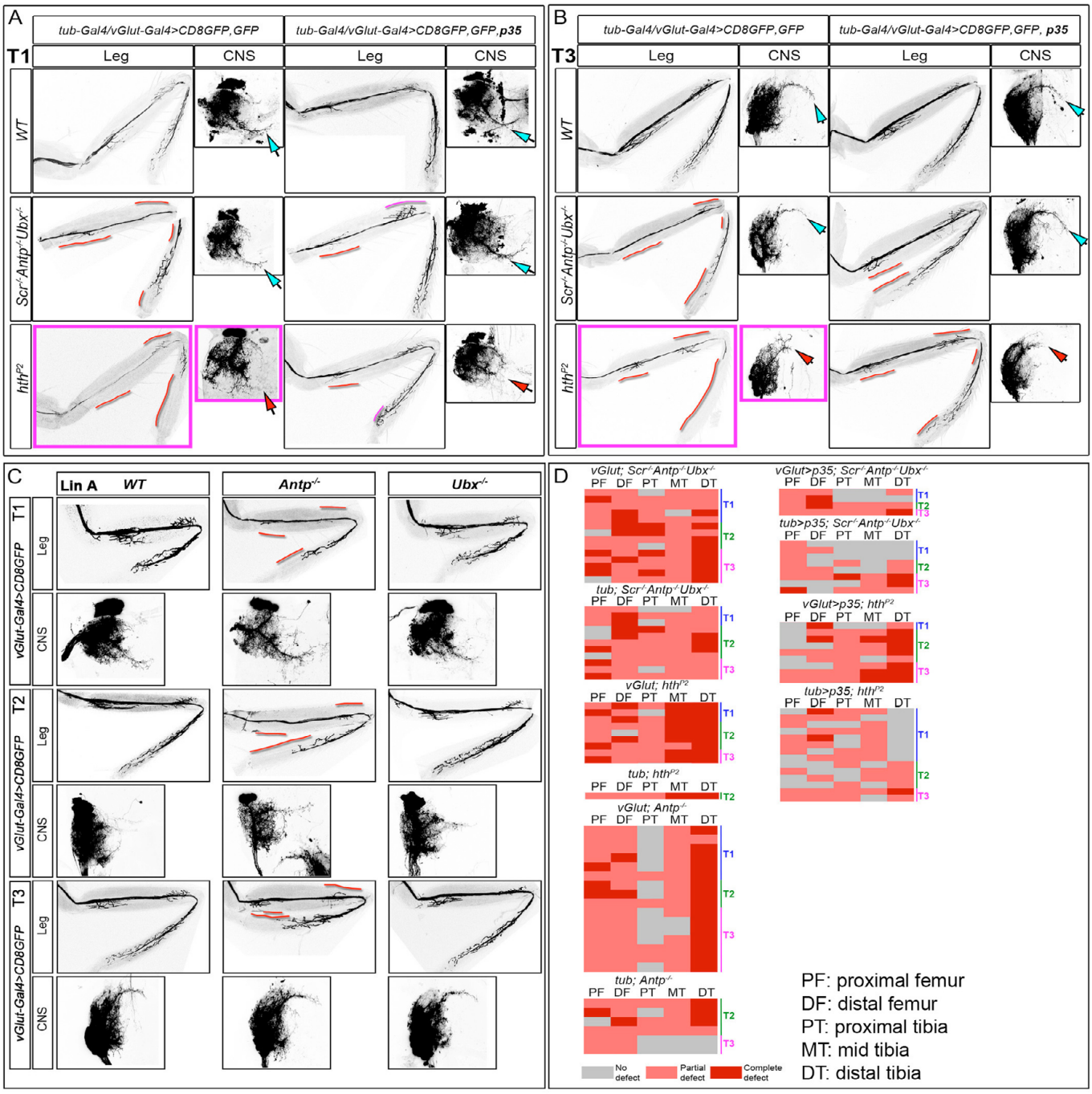

Fig. S5. Aberrant axon branching and dendritic morphologies in Hox and *hth* mutant LinA MNs. (**A**,**B**) Aberrant axon branching and dendritic morphologies in Hox and *hth* mutant T1 (A) and T3 (B) LinA MNs. All panels show axons and dendrites of adult stage LinA MARCM clones in T1 labeled with *tub-Gal4*; *vGlut-Gal4 >CD8GFP* except hth^{P2} clones, which are labeled with only *vGlut-Gal4 >CD8GFP* (pink boxes). Hox and *hth* mutant LinA MNs have axon-targeting defects (red bars). Ectopic expression of p35 partially rescues the axonal targeting phenotypes and generates ectopic axonal targeting (pink bars), for both Hox and *hth* mutant clones. *hth* mutant clones also show a lack of midline-crossing dendrites (light-blue versus red arrows). (**C**) Axon-targeting defects in *Antp* and *Ubx* mutant LinA MNs. All panels show axons in adult legs of LinA MARCM clones labeled with *vGlut-Gal4 >CD8GFP*. Shown are examples of T1 (top), T2 (middle) and T3 (bottom) legs. From left to right: WT, $Antp^{-/-}$ and $Ubx^{-/-}$ LinA MN clones. *Antp* mutant LinA MNs have axon-targeting defects in all three segments (red lines). *Ubx* mutant LinA clones have normal axon targeting in all three segments. (**D**) Spatial distribution of Hox and *hth* MN axon-targeting defects. LinA clones were labeled with *tub-Gal4; vGlut-Gal4 >CD8GFP* or *vGlut-Gal4 >CD8GFP*. Adult stage axon targeting was scored as follows: gray boxes (WT axon branching), pink boxes (partial absence of branches) and red boxes (complete absence of branches). Each row represents an individual LinA MARCM clone. Leg regions normally targeted by LinA MNs are labeled above each panel (PF, proximal femur; DF, distal femur; PT, proximal tibia; MT, mid tibia; DT, distal tibia). Segmental positions of the clones are labeled on the right (T1, T2 and T3).

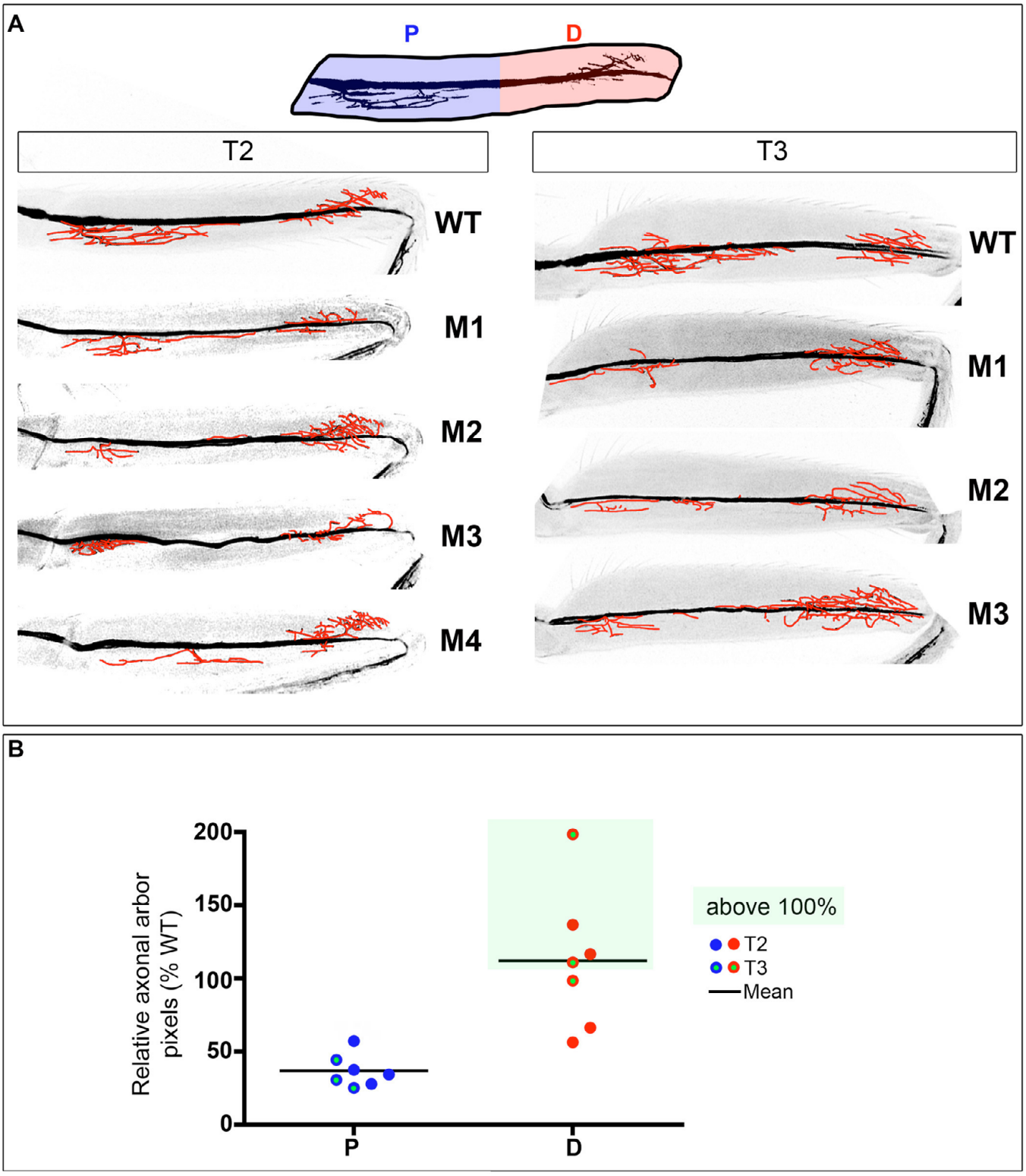

Fig. S6. Quantification of the instructive role of Antp levels. (**A**) Examples in T2 (left) and T3 (right) of LinA MN MARCM clones expressing either GFP (WT) or Antp (M1-M4) via the *vGlut-Gal4* driver. Blue and pink shaded regions highlight the proximal femur (P) and distal femur (D). Axonal arbors (red) were traced in merged images using Photoshop, which were used for quantification in B. (**B**) Quantification of axonal arbors in individual LinA clones. Each point represents the relative pixel numbers compared with the WT LinA clones. There was severe reduction in axonal arbors in the proximal femur; by contrast, in 4/7 samples, more axonal arbors were formed in the distal femur.

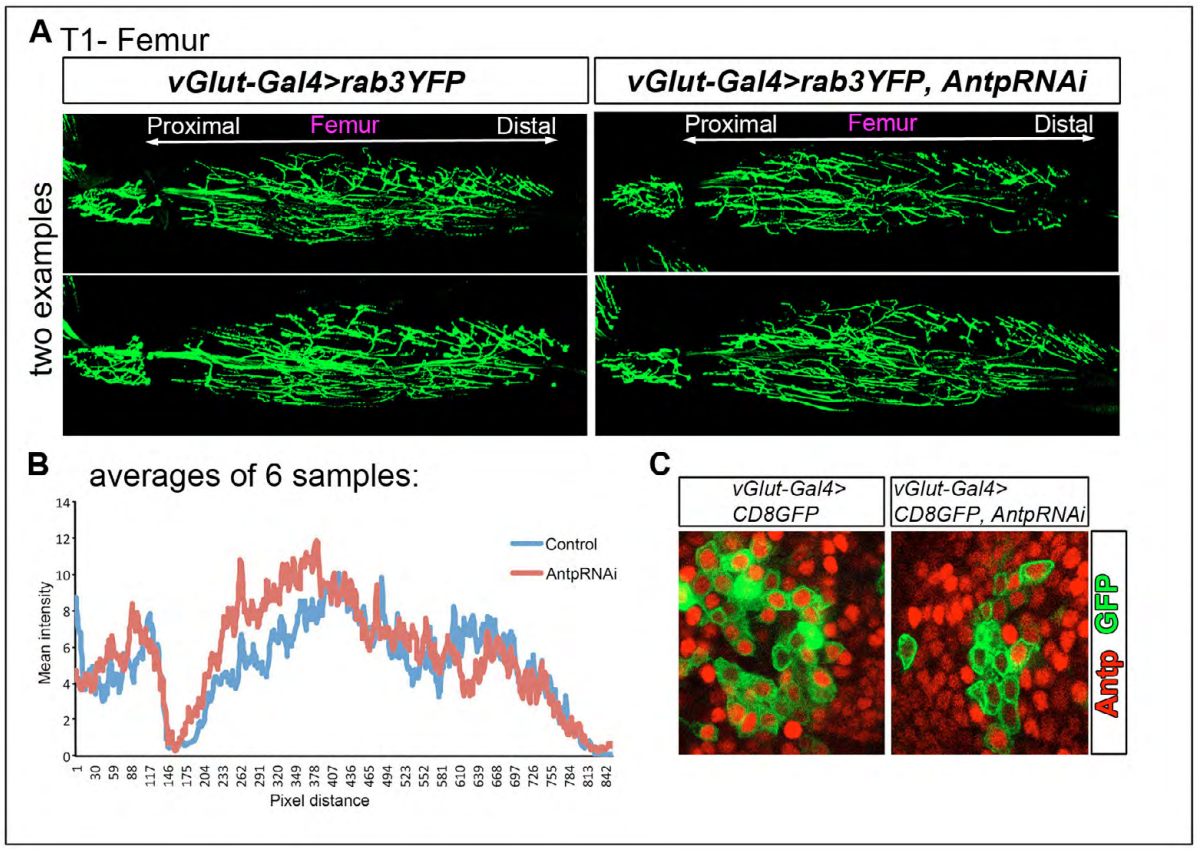

Fig. S7. Knocking down Antp levels produces a distal-to-proximal shift in axon targeting. (**A**) Two examples each of T1 femurs in which all MNs express either *rab3YFP* (left) or *rab3YFP+AntpRNAi* (right) under the control of the *vGlut-Gal4* driver. To increase the RNAi efficiency, animals were raised at 29°C. Note that all motoneurons, not only those derived from LinA, are labeled in this experiment. Proximal is left and distal is right. (**B**) Quantification of axonal arbors in the adult T1 femur. Each curve represents the average YFP intensity of six samples summing all signal from the proximal (left) to distal (right) femur. In the *AntpRNAi* specimens, there was a reduction in axonal arbors in the distal femur and more axonal arbors were observed in the proximal femur. (**C**) *AntpRNAi* validation. The images show examples of *vGlut >CD8GFP* (green) cells either without (left) or also expressing (right) *AntpRNAi*. In addition to GFP, these preparations were stained for Antp (red). Note the reduction in Antp levels compared with the surrounding (non-*vGlut*-expressing) cells in the *vGlut >CD8GFP; AntpRNAi* image compared with the *vGlut >CD8GFP* image. To quantify these knockdowns further, Antp levels were measured (using ImageJ) in both *vGlut*-expressing and -nonexpressing cells. These quantifications reveal that *vGlut >AntpRNAi* resulted in a ~25–30% reduction in Antp levels compared with the control (data not shown). As these measurements were carried out at 25°C, they are likely to represent an underestimate of the knockdowns in the experiment shown in panels A and B, which were carried out at 29°C.

Table S1. Summary of mutant single-cell MARCM clones

Seg-ment		*Scr*$^{-/-}$ *Antp*$^{-/-}$ *Ubx*$^{-/-}$ (*n*=87)						*hth*^{P2} (*n*=38)					
		Axon defect	Dendrite defect				Total	Axon defect	Dendrite defect				Total
		Aberrant or absence of termini	Midline crossing*	Close to midline‡	Less territory	Segment boundary crossing		Aberrant or absence of termini	Midline crossing*	Close to midline‡	Less territory	Segment boundary crossing	
Coxa	T1	0/10	0/10	1/10	1/10	0/10	1/10	3/12	2/12	4/12	6/12	4/12	10/12
	T2	N/A	N/A	N/A	N/A	N/A	N/A	N/A	N/A	N/A	N/A	N/A	N/A
	T3	N/A	N/A	N/A	N/A	N/A	N/A	N/A	N/A	N/A	N/A	N/A	N/A
Tro	T1	0/2	0/2	2/2	0/2	0/2	2/2	N/A	N/A	N/A	N/A	N/A	N/A
	T2	0/1	0/1	0/1	0/1	0/1	0/1	N/A	N/A	N/A	N/A	N/A	N/A
	T3	N/A	N/A	N/A	N/A	N/A	N/A	N/A	N/A	N/A	N/A	N/A	N/A
Prox. femur	T1	6/8	2*/8	0/8	0/8	0/8	8/8	5/6	0/6	0/6	5/6	0/6	5/6
	T2	5/7	3/7	2/7	2/7	0/7	6/7	0/1	0/1	0/1	0/1	0/1	0/1
	T3	1/2	0/2	0/2	0/2	0/2	1/2	N/A	N/A	N/A	N/A	N/A	N/A
Distal femur	T1	3/6	3/6	0/6	2/6	0/6	6/6	0/3	3/3	0/3	1/3	0/3	3/3
	T2	1/8	5/8	0/8	5/8	0/8	7/8	1/2	2/2	0/2	1/2	0/2	2/2
	T3	0/3	0/3	0/3	0/3	0/3	0/3	N/A	N/A	N/A	N/A	N/A	N/A
Prox. tibia	T1	0/2	0/2	1/2	0/2	0/2	1/2	1/3	2*/3	1/3	0/3	0/3	3/3
	T2	0/5	1*/5	3/5	1/5	0/5	5/5	0/1	0/1	1/1	0/1	0/1	1/1
	T3	N/A	N/A	N/A	N/A	N/A	N/A	0/2	2*/2	0/2	1/2	0/2	2/2
Mid tibia	T1	1/13	7/13	2/13	6/13	0/13	9/13	0/3	0/3	0/3	0/3	0/3	0/3
	T2	1/6	2/6	0/6	1/6	0/6	3/6	0/3	0/3	0/3	0/3	0/3	0/3
	T3	0/1	0/1	0/1	0/1	0/1	0/1	N/A	N/A	N/A	N/A	N/A	N/A
Distal tibia	T1	0/4	0/4	1/4	0/4	0/4	1/4	N/A	N/A	N/A	N/A	N/A	N/A
	T2	0/8	2/8	1/8	1/8	0/8	4/8	0/2	0/2	2/2	0/2	0/2	2/2
	T3	0/1	0/1	1/1	0/1	0/1	1/1	N/A	N/A	N/A	N/A	N/A	N/A
Total	T1	10/45	12/45	7/45	9/45	0/45	55/87	9/27	7/27	5/27	12/27	4/27	28/38
	T2	7/35	13/35	6/35	10/35	0/35		1/9	2/9	3/9	1/9	0/9	
	T3	1/7	0/7	1/7	0/7	0/7		0/2	2/2	0/2	1/2	0/2	
	Total	18/87	25/87	14/87	19/87	0/87		10/38	11/38	7/38	13/38	4/38	
	Key:	<25%	>25% and <50%	>50%									

*'Midline crossing' refers to either the absence (*) of normally crossing dendrites or dendrites that aberrantly cross the midline.
‡'Close to midline' refers to the presence of dendrites that aberrantly approach, but do not cross, the midline.
N/A, sample was not obtained.